

## First-principle study on the optical properties of TiO<sub>2</sub> doped with different Lu contents

J. H. Luo<sup>a,\*</sup>, L. J. Xiang<sup>b</sup>, L. S. Chen<sup>a</sup>, Y. Li<sup>a</sup>

<sup>a</sup>*College of Materials Science and Engineering, Yangtze Normal University, Chongqing 408100, PR China*

<sup>b</sup>*School of Mechatronic Engineering, Guangdong Polytechnic Normal University, Guangzhou 510665, PR China*

Compared to pure TiO<sub>2</sub>, Lu-doped TiO<sub>2</sub> shows enhanced photocatalytic performance in the visible light range. In order to investigate the influence of Lu doping contents on optical properties of Lu-doped TiO<sub>2</sub>, we conducted first-principle on TiO<sub>2</sub> with different contents of Lu doping. The results indicate that as the contents of Lu increases, the band gap of Lu-doped TiO<sub>2</sub> gradually decreases. Within the visible light range, Lu-doped TiO<sub>2</sub> exhibits an expanded absorption band ranging from 450 nm to 600 nm. Furthermore, when the Lu contents reaches 9.09 at%, the absorption intensity shows a higher value between 700 nm and 800 nm. Lu-doped TiO<sub>2</sub> demonstrates a low reflectance in the visible light region, with the maximum reflectance occurring in the infrared region at approximately 65%. The calculated dielectric constant results suggest that the probability of electronic absorption of photons in Lu-doped TiO<sub>2</sub> initially decreases and then increases with an increase in Lu contents.

(Received September 22, 2023; Accepted December 14, 2023)

**Keywords:** Lu-doped TiO<sub>2</sub>, Band structure, Dielectric function, Absorption, Reflection

### 1. Introduction

TiO<sub>2</sub> is widely used as a photocatalyst for the photodegradation of organic pollutants under UV irradiation [1, 2]. However, the photocatalytic efficiency of anatase TiO<sub>2</sub> is small under visible irradiation due to its large band gap of 3.2 eV. Applications of pure TiO<sub>2</sub> is greatly limited. Doping with other elements is considered to be an effective method for reducing the band gap and enhancing the photocatalytic efficiency of TiO<sub>2</sub> [3–7]. For instance, Solanki [8] studied the band gap of metal (Co, Pd, Ni) doped TiO<sub>2</sub>, and the results shows that the band gap of Co-doped TiO<sub>2</sub>, Pd-doped TiO<sub>2</sub> and Ni-doped TiO<sub>2</sub> are 3.07 eV, 2.90 eV and 2.81 eV, respectively, which were lower than that of TiO<sub>2</sub>. Zulkifli et al [9] found that the Al-doped TiO<sub>2</sub> has the highest photocatalytic performance for degradation of 10 ppm methylene blue solution within 60 minutes.

In terms of the theoretical calculations, the optical properties of doped TiO<sub>2</sub> are mainly calculated by first-principle [10–13], so as to further explain the experimental phenomena. At present, the calculation of doped TiO<sub>2</sub> mainly focuses on the optical properties, including energy band structure, total or partial densities of state, absorption spectrum, reflectance spectrum and so on [14–17]. The calculation results also show that the doped TiO<sub>2</sub> has lower band gap and better light absorption intensity in the visible range [18, 19].

---

\* Corresponding author: 20170128@yznu.edu.cn  
<https://doi.org/10.15251/JOR.2023.196.775>

In our previous study [20], the optical properties of Lu-doped  $\text{TiO}_2$  thin film were investigated. Using the tangent method, the band gap of Lu-doped  $\text{TiO}_2$  film was estimated to be approximately 2.9 eV. The Lu-doped  $\text{TiO}_2$  demonstrated favorable light absorption in the visible light range, specifically between 400 and 450 nm. Under natural light conditions, the Lu-doped  $\text{TiO}_2$  thin film effectively degraded methyl orange solution after 72 hours of exposure. In this work, the first-principle were used to investigate the influence of Lu contents on optical properties of Lu-doped  $\text{TiO}_2$ .

## 2. Model construction and calculation methods

### 2.1. Model construction

The unit cell of anatase  $\text{TiO}_2$  is extended to a  $2 \times 2 \times 1$  supercell molecular structure, as shown in Fig. 1a, with red representing O atoms and gray representing Ti atoms. One Ti atom in Fig. 1a is then replaced with the rare earth element Lu, forming the Lu-doped  $\text{TiO}_2$  molecular model depicted in Fig. 1a. Another Ti atom is also replaced, resulting in the model shown in Fig. 1b. Fig. 1c and d represent the Lu-doped  $\text{TiO}_2$  molecular models formed by replacing 3 and 4 Ti atoms with Lu atoms, respectively. After these additions, the Lu atomic percentage in the resulting models corresponds to 2.27 at%, 4.55 at%, 6.82 at%, and 9.09 at%, respectively.

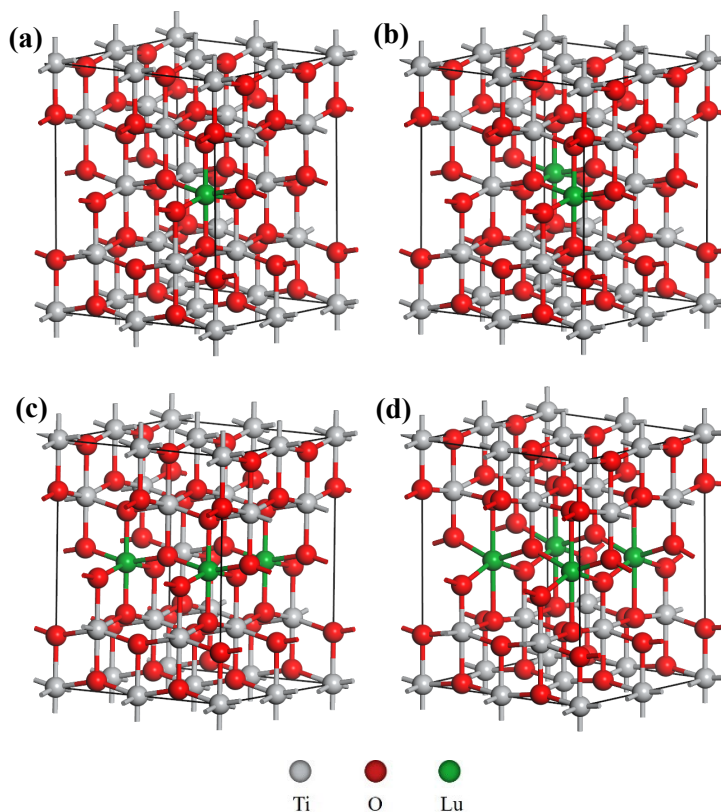


Fig. 1. Molecular models of Lu-doped  $\text{TiO}_2$ . (a) 2.27 at%; (b) 4.55 at%; (c) 6.82 at%; (d) 9.09 at%.

## 2.2. Calculation methods

The first-principle was carried out using Materials Studio 7.0. Structural optimization of Lu-doped  $\text{TiO}_2$  molecular models were performed using the generalized gradient approximation (GGA) with the Perdew–Burke–Ernzerh (PBE) theory [21] and a cutoff energy of 380 eV. The optimized models were used for band structure and optical property calculations to analyze the effects of different Lu doping contents on the material's optical properties.

## 3. Results and discussion

### 3.1. Band structure

Fig. 2 shows the calculated band structures and corresponding partial density of states (PDOS) for different Lu-doped  $\text{TiO}_2$  molecular models. The left side represents the results of the band structure calculations, while the right side shows the local distribution of electronic states at specific energies.

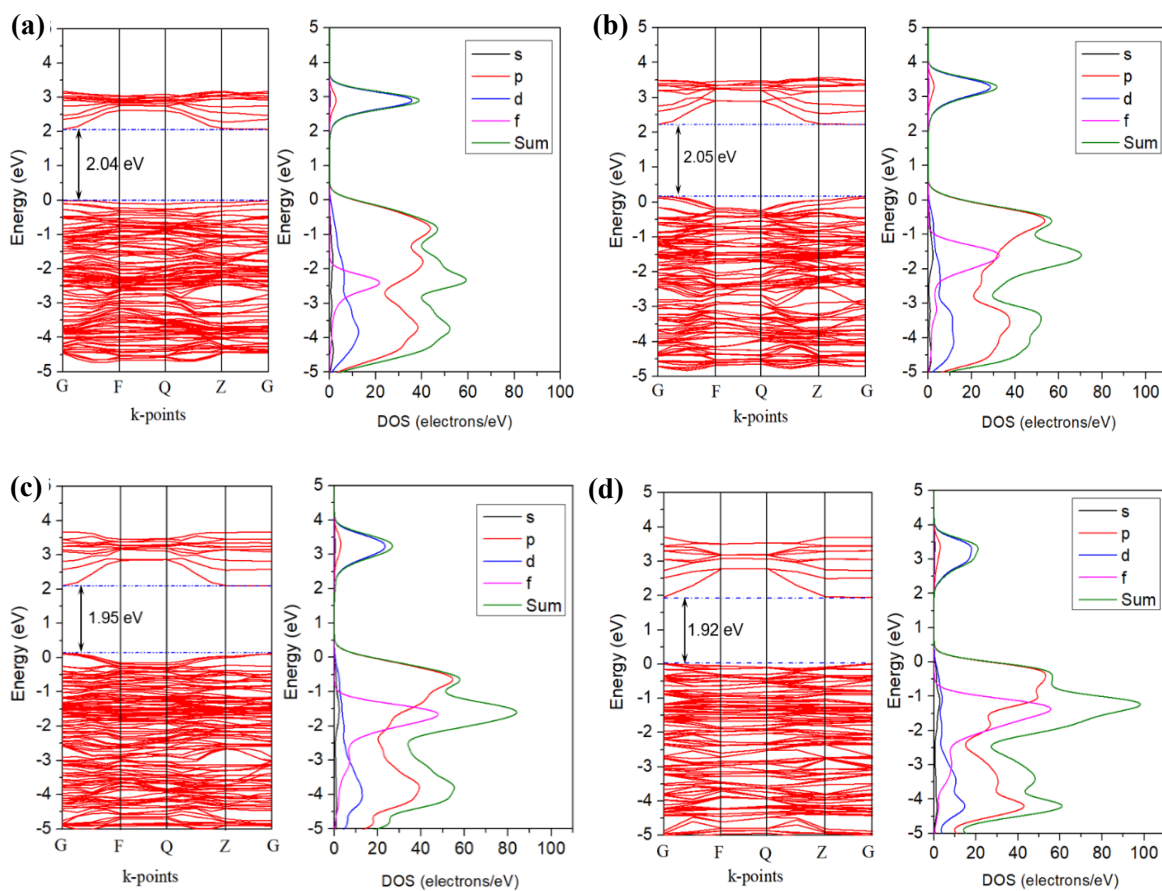


Fig. 2. Calculated results for the band structure and local PDOS of  $\text{TiO}_2$  doped with different Lu contents. (a) 2.27 at%, (b) 4.55 at%, (c) 6.82 at%, and (d) 9.09 at%.

Fig. 2a on the left side presents the band structure of the  $\text{TiO}_2$  molecular model with a Lu doping content of 2.27 at%. The band gap is observed to be 2.04 eV. A significant decrease in the band gap is evident compared to the calculated result of 2.12 eV [22, 23] or 2.15 eV [24] for pure  $\text{TiO}_2$ . However, it should be noted that this result is lower than the experimental value of 2.9 eV [20]. This discrepancy can be attributed to the fact that the theoretical calculations are based on idealized materials. Additionally, the GGA method used in density functional theory calculations often underestimates the band gap of metal oxides. As a result, the calculated band gaps are generally lower. Nevertheless, these deviations do not affect the relative analysis of the electronic structure. Fig. 2a on the right side displays the corresponding PDOS, revealing that the conduction band minimum and valence band maximum are formed by the hybridization of Ti-3d and O-2p states. The Ti-3d states play a significant role in the conduction band minimum, while the O-2p states dominate the valence band maximum. The energy difference between the valence band maximum and the Fermi level is approximately 3.2 eV.

Fig. 2b on the left side shows the calculated band structure of the  $\text{TiO}_2$  molecular model with a Lu doping content of 4.55 at%. It can be observed that the band gap is 2.05 eV, which is similar to the result in Fig. 2a. However, there is an increase in the Lu-4f state peak in the energy range of -1 to -0.5 eV in the valence band.

Fig. 2c presents the calculated results for the band structure and density of states distribution of the  $\text{TiO}_2$  molecular model with a Lu doping content of 6.82 at%. It is found that the band gap starts to decrease, reaching 1.95 eV. Compared to the  $\text{TiO}_2$  models doped with Lu contents of 2.27 at% and 4.55 at%, the decrease is 0.1 eV. From the density of states distribution in Fig. 2c, it can be observed that with the increase in Lu doping contents, the overlap region of Lu-4f with Ti-3d and O-2s states increases. This causes a shift in the valence band maximum, eventually crossing the Fermi level (0 eV), resulting in a decrease in the band gap.

Fig. 2d displays the calculated results for the band structure and density of states distribution of the  $\text{TiO}_2$  molecular model with a Lu doping content of 9.09 at%. It is observed that the band gap further decreases, reaching 1.92 eV. From the density of states distribution in Fig. 2d, it can be seen that the Lu-4f state peak increases significantly, reaching its maximum value. The overlap region of Lu-4f with Ti-3d and O-2s states increases, leading to an expanded energy range, which causes a further shift in the valence band maximum.

### 3.2. Absorption and reflection properties

Fig. 3 shows the optical absorption spectra of Lu-doped  $\text{TiO}_2$ . Similar to pure  $\text{TiO}_2$ , it exhibits strong absorption in the ultraviolet region (200–400 nm). The intrinsic  $\text{TiO}_2$  absorbs visible light within a range of approximately 380 nm [8, 18, 25–27]. After introducing Lu doping, the absorption tail in the visible light range extends from 380 nm to between 450 nm and 600 nm, with the highest absorption ability observed at a Lu content of 2.27 at%. Additionally, the absorption intensity in the visible light range decreases with increasing Lu contents. However, when the Lu contents reaches 9.09 at%, the absorption intensity starts to increase again, especially between 700 nm and 800 nm, showing a significant increase. This trend is consistent with the previously mentioned band structure calculation results. At this Lu content, the band gap is minimized at 1.92 eV, which facilitates the absorption of light by the valence band electrons, enabling their transition to the conduction band.

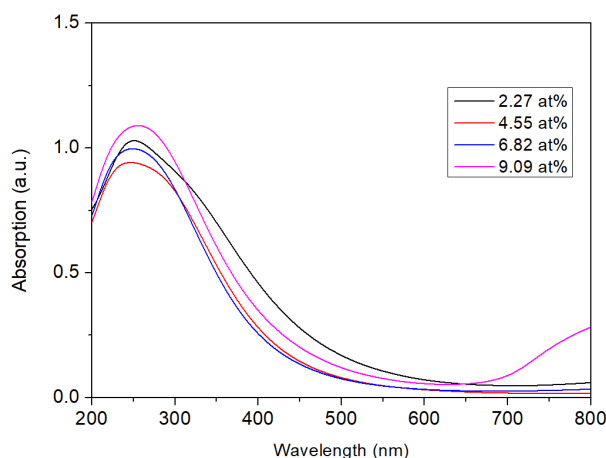


Fig. 3. Optical absorption spectrum of  $\text{TiO}_2$  doped with different Lu contents.

Fig. 4 represents the optical reflectance spectrum of Lu-doped  $\text{TiO}_2$ . From the graph, it can be observed that the optical reflectance in the infrared region ( $<1.58$  eV) reaches its highest value of 60% when the Lu content reaches 9.09 at%. For other Lu contents, the reflectance decreases with increasing Lu contents. In the visible light region (1.58-3.25 eV) and the ultraviolet region ( $>3.25$  eV), the reflectance remains relatively low. Overall, doping increases the reflectance in the infrared region, with the maximum reflectance reaching approximately 65%.

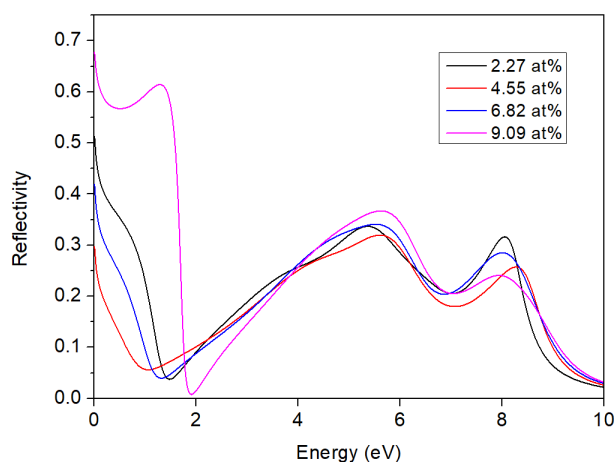


Fig. 4. Optical reflectance spectrum of  $\text{TiO}_2$  doped with different Lu contents

### 3.3. Dielectric function

Fig. 5a illustrates the real part of the dielectric function curves for  $\text{TiO}_2$  doped with varying Lu contents. The vertical axis represents the static dielectric constant, reflecting the material's polarization capacity under an external electric field. A higher static dielectric constant indicates a stronger ability to bind charges. The graph reveals non-uniform variations in the static dielectric constants, with respective values of 33.66, 9.79, 20.28, and 96.50. Notably, when the Lu content reaches 9.09 at%, the system demonstrates significantly superior charge binding capability

compared to other compositions. As the incident light energy increases, the dielectric constants tend to decline, aside from a pronounced peak near 2.8 eV, while the remaining energy regions exhibit no substantial changes.

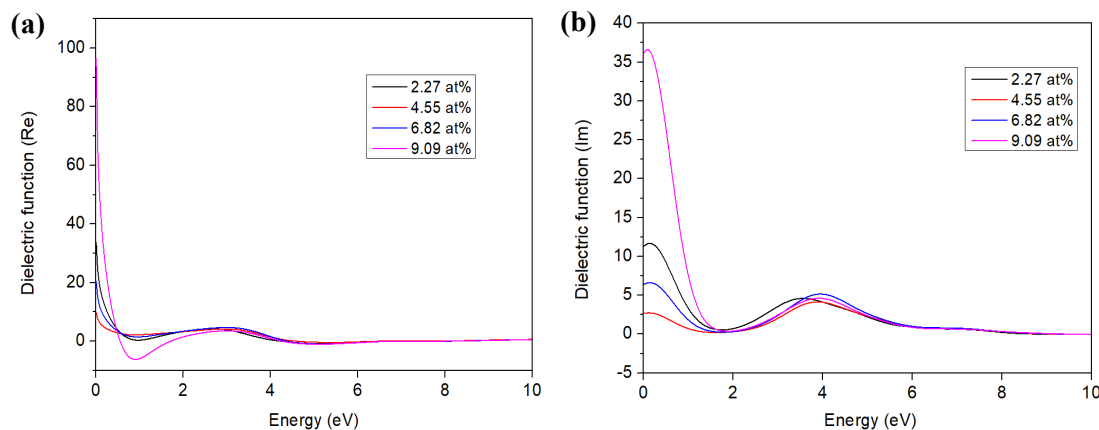


Fig. 5. Dielectric function of TiO<sub>2</sub> doped with different Lu contents. (a) Real part and (b) Imaginary part.

Fig. 5b presents the imaginary part of the dielectric function curve. The dielectric constant signifies the material's response to an external electric field and, on a microscopic scale, signifies the formation of numerous electric dipoles. The imaginary part characterizes the energy dissipation associated with electric dipole formation and relates to interband transitions. A larger imaginary part value implies a heightened degree of electron excitation and transition, reflective of inferior insulation performance and an increased probability of electron-photon absorption. Greater electron population in the excited state corresponds to an increased probability of subsequent transitions. With increasing doping contents, the four systems exhibit secondary peaks at 3.58 eV, 3.87 eV, 3.96 eV, and 3.91 eV. These peaks arise from electron transitions between Ti-3d, O-2p, and Lu-4f states and their intensity strengthens with higher doping contents, indicating an increased probability of electron-photon absorption and a greater number of electrons in the excited state, consequently amplifying the probability of the subsequent transition.

#### 4. Conclusions

In summary, the band structure, absorption and reflection properties, dielectric function of Lu-doped TiO<sub>2</sub> were calculated by the GGA approach. First, we study the influence of four different Lu doping contents of 2.27 at%, 4.55 at%, 6.82 at% and 9.09 at% on the band structure of Lu-doped anatase TiO<sub>2</sub>, and find that the band gap value decreases gradually with the doping contents increasing. Second, we study the absorption and reflection properties of Lu-doped TiO<sub>2</sub>, and the results indicated that doping Lu element can increase absorption in the visible and the reflectance in the infrared region. At last, the dielectric function of Lu-doped TiO<sub>2</sub> was calculated, and the results show that as the doping contents increase, the probability of electrons absorbing photons increases. Thus, these results demonstrate that the Lu-doped TiO<sub>2</sub> may be beneficial for improving the photocatalytic activity.

## References

- [1] M. I. Kanjal, M. Muneer, M. Saeed, W. Chu, N. Alwadai, M. Iqbal, A. Abdelhaleem, Ara. J. Chem. 15(9), 104061 (2022); <https://doi.org/10.1016/j.arabjc.2022.104061>
- [2] R. Kumar, A. K. Singh, P. S. Mondal, Materials Today: Proceedings, 66(7), 3244–3249 (2022); <https://doi.org/10.1016/j.matpr.2022.06.257>
- [3] Y. Mingmongkol, D. T. T. Trinh, P. Phuinthiang, D. Channei, K. Ratananikom, A. Nakaruk, W. Khanitchaidecha, Nanomaterials, 12, 1198 (2022); <https://doi.org/10.3390/nano12071198>
- [4] B. Zhang, H. Wang, J. Luo, S. Liu, Y. Tian, J. Electroanal. Chem. 930, 117159 (2023); <https://doi.org/10.1016/j.jelechem.2023.117159>
- [5] S. Muthukrishnan, R. Vidya, A. O. Sjästad, Mater. Chem. Phys. 299, 127467 (2023); <https://doi.org/10.1016/j.matchemphys.2023.127467>
- [6] G. Bahmanrokh, C. Cazorla, S. S. Mofarah, R. Shahmiri, Y. Yao, I. Ismail, W. Chen, P. Koshy, C. C. Sorrell, Nanoscale, 12, 4916–4934 (2020); <https://doi.org/10.1039/C9NR08604H>
- [7] B.-G. Park, Gels, 8, 14 (2022); <https://doi.org/10.3390/gels8010014>
- [8] K. Solanki, D. Parmar, C. Savaliya, S. Kumar, S. Jethva, Materials Today: Proceedings, 50, 2576–2580 (2022); <https://doi.org/10.1016/j.matpr.2021.10.182>
- [9] R. C. Zulkifli, F. Azaman, M. H. Razali, A. Ali, M. A. A. M. Nor, Dig. J. Nanomater. Bio. 18(1), 243–252 (2023); <https://doi.org/10.15251/DJNB.2023.181.243>
- [10] B. Nazir, U. Rehman, S. Arshad, M. I. Arshad, N. Sabir, M. A. Javid, F. Iqbal, M. A. Nabi, Materials Today: Proceedings, 47, S94–S98 (2021); <https://doi.org/10.1016/j.matpr.2020.05.529>
- [11] S. M. Rasul, D. R. Saber, S. B. Aziz, Results Phys. 38, 105688 (2022); <https://doi.org/10.1016/j.rinp.2022.105688>
- [12] X. Lang, X. Liu, J. Xue, D. Li, L. Cao, H. Zhang, Physica B, 624, 413443 (2022); <https://doi.org/10.1016/j.physb.2021.413443>
- [13] Y. Wang, X. Wang, L. Li, Y. Wu, Mater. Lett. 307, 131000 (2022); <https://doi.org/10.1016/j.matlet.2021.131000>
- [14] D. Xia, Q. Hou, Y. Guan, Z. Xu, M. Chen, Chem. Phys. 539, 110949 (2020); <https://doi.org/10.1016/j.chemphys.2020.110949>
- [15] F. Saidi, A. Mahmoudi, K. Laidi, T. Hidouri, S. Nasr, Comput. Condens. Matte. 28, e00576 (2021); <https://doi.org/10.1016/j.cocom.2021.e00576>
- [16] A. Hussain, A. Rauf, E. Ahmed, M. S. Khan, S. A. Mian, J. Jang, Molecules, 28, 3252 (2023); <https://doi.org/10.3390/molecules28073252>
- [17] H. Ye, G. Zuo, Y. Cao, Chem. Phys. Lett. 828, 140720 (2023); <https://doi.org/10.1016/j.cplett.2023.140720>
- [18] Z. Ma, F. Ren, Z. Yang, A. A. Volinsky, Optik, 241, 167107 (2021); <https://doi.org/10.1016/j.ijleo.2021.167107>
- [19] A. Soussi, A. Elfanaoui, A. Ait hssi, M. Taoufiq, A. Asbayou, L. Boulkaddat, N. Labchir, R. Markazi, A. Ihlal, K. Bouabid, Mater. Today Commun. 36, 106520 (2023); <https://doi.org/10.1016/j.mtcomm.2023.106520>
- [20] Ji-hui. Luo, Mater. Sci.–Medzg. 28(4), 383–387 (2022); <https://doi.org/10.5755/j02.ms.29676>
- [21] B. Hammer, L. B. Hansen, J. K. Nørskov, Phys. Rev. B, 59(11), 7413–7421 (1999); <https://doi.org/10.1103/PhysRevB.59.7413>
- [22] Z. Zeng, M. Xu, Y. Sun, J. Xu, Y. Zhong, Optik, 261, 169231 (2022);

<https://doi.org/10.1016/j.ijleo.2022.169231>

[23] M. Khan, J. Xu, N. Chen, W. Cao, J. Alloy Compd. 513, 539–545 (2012);

<https://doi.org/10.1016/j.jallcom.2011.11.002>

[24] S. Liu, B. Liu, T. Wang, S. Zhu, Y. Li, Phys. Scr. 98, 015827 (2023);

<https://doi.org/10.1088/1402-4896/aca74>

[25] H. Xing, L. Wu, X. Li, Int. J. Electrochem. Sci. 17, 22066 (2022);

<https://doi.org/10.20964/2022.05.32>

[26] M. Jahdi, S. B. Mishra, E. N. Nxumalo, S. D. Mhlanga, A. K. Mishra, Opt. Mater. 104, 109844 (2020); <https://doi.org/10.1016/j.optmat.2020.109844>

[27] M. Tong, Y. Chen, T. Wang, S. Lin, G. Li, Q. Zhou, R. Chen, X. Jiang, H. Liao, C. Lu, Molecules, 28, 2433 (2023); <https://doi.org/10.3390/molecules28062433>